Int. J. Heat Mass Transfer. Vol. 13, pp. 647–650. Pergamon Press 1970. Printed in Great Britain

SHORTER COMMUNICATIONS

THE SOLUTION OF RADIATIVE EXCHANGE PROBLEMS BY LEAST SQUARES TECHNIQUES

E. M. SPARROW
University of Minnesota, Minneapolis, Minnesota

and

A. HAJI-SHEIKH
University of Texas at Arlington, Arlington, Texas

(*Received* 9 *December* 1968 *and in revised form* 17 *September* 1969)

GENERAL FORMULATION

COMPUTATIONAL experiments are reported herein to illustrate a solution method which satisfies the governing integral equations of radiant interchange in the least squares sense. The problems with which we are concerned are governed by one or more linear integral equations of the type

$$f_i(x_i, y_i, z_i) = F_i(x_i, y_i, z_i) + \sum_{j=1}^{N} \gamma_{ij} \int_{A_j} f_j(x_j, y_j, z_j)\, K(x_i, \ldots, z_j)\, \mathrm{d}A_j \qquad (1)$$

$i = 1, 2, \ldots, N$. The f functions may represent either the radiosity B, the temperature T, or the local heat flux q (e.g. [1] Chapter 3). The F_i denote known functions and the γ_{ij} are known constants; the $K\,\mathrm{d}A_j$ are angle factors. To begin the solution, each of the f_k is expressed as a sum of preassigned functions, that is

$$f_k(x_k, y_k, z_k) = \sum_{m=1}^{M_k} C_{km}\, g_{km}(x_k, y_k, z_k), \qquad k = 1, 2, \ldots, N. \qquad (2)$$

The g_{km} are selected using all available insights, for instance, symmetry, limiting conditions, and so forth. The C_{km} are yet to be determined.

The f_k are introduced into the right-hand side of equation (1) and the indicated integrations are performed, either analytically (wholly or in part) or numerically as a subroutine of the general computer program. Let the participating integrals be denoted by

$$\overset{(i)}{\underset{jm}{\Omega}} = \int_{A_j} g_{jm}(x_j, y_j, z_j)\, K(x_i, \ldots, z_j)\, \mathrm{d}A_j. \qquad (3)$$

Then, after introducing the representation (2) for f_i into the left-hand side of (1) and making use of (3), the governing integral equations (1) reduce to a set of algebraic equations

$$\sum_{m=1}^{M_i} C_{im}\left(g_{im} - \gamma_{ii} \overset{(i)}{\underset{im}{\Omega}}\right) - \sum_{\substack{j=1 \\ (j \neq i)}}^{N} \gamma_{ij} \left[\sum_{m=1}^{Mj} C_{jm} \overset{(i)}{\underset{jm}{\Omega}}\right] = F_i \qquad (4)$$

$i = 1, 2, \ldots N$; in which the g, Ω, and F are functions of position x_i, y_i, z_i.

The set of equations (4) contains $M_1 + M_2 + \ldots M_N = \tilde{M}$ unknown coefficients C. To find the C, one proceeds as follows: The algebraic equations (4) are evaluated at a total of P discrete positions on the participating surfaces such that $P \geqslant \tilde{M}$, giving P linear algebraic equations for the $\tilde{M}$ unknown values of C. This mathematical system is dealt with using least squares techniques. In particular, it has been found highly convenient to employ the orthonormalization subroutine,* which automatically constructs orthonormal functions and, with these functions, determines the numerical values of the coefficients C. All local results of interest follow directly once the f_k are found. For instance, if f corresponds to the radiosity B, then the local heat flux for a gray diffuse surface is given by

$$q = \varepsilon(\sigma T^4 - B)/(1 - \varepsilon). \qquad (5)$$

COMPUTATIONAL EXPERIMENTS

One-dimensional systems. Consider the parallel plate system shown at the upper left of Fig. 1. The parallel surfaces have the same uniform temperature T and the same graybody emittance ε, and the external environment contains black body radiation at temperature T_e. The governing integral equation for the radiosity is readily derived as

* The orthonormalization subroutine is listed in the COOP manual as E2 UOFM ORTHON. A listing of the program can also be obtained from the authors.

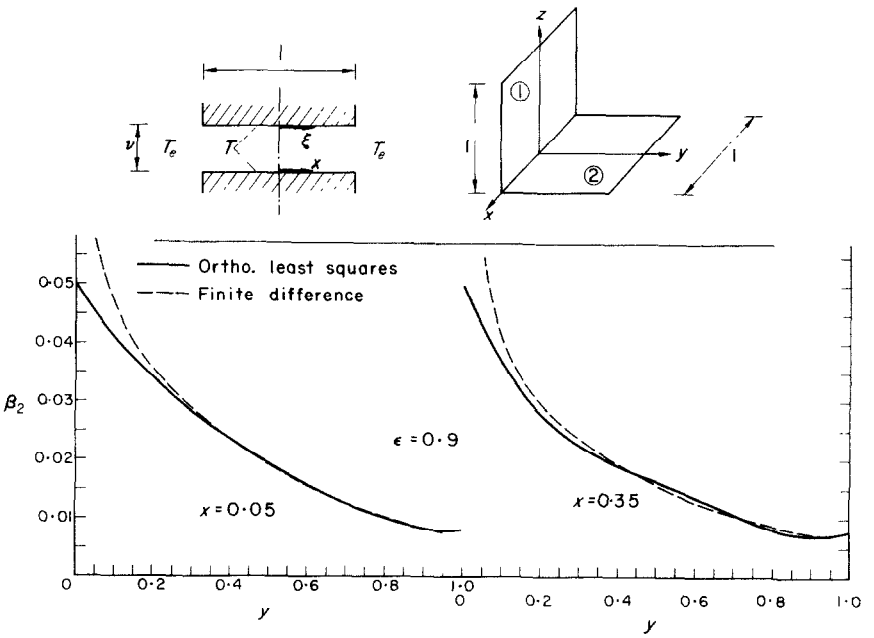

FIG. 1. Radiosity distributions, second computational experiment, $\varepsilon = 0.9$.

$$\beta(x) = 1 + (1 - \varepsilon) \int_{-\frac{1}{2}}^{\frac{1}{2}} \beta(\xi) \frac{v^2/2}{[(x - \xi)^2 + v^2]^{\frac{3}{2}}} \, d\xi \qquad (6)$$

in which $\beta = (B - \sigma T_e^4)/\varepsilon\sigma(T^4 - T_e^4)$ and B is the radiosity. In view of the symmetry in x, solutions are proposed in the form

$$\beta(x) = \sum_{m=1}^{M} C_m x^{2(m-1)}, \qquad \beta(\xi) = \sum_{m=1}^{M} C_m \xi^{2(m-1)}. \qquad (7)$$

The C_m were found by employing the orthonormalization least squares procedure as outlined above, wherein the participating integrals were evaluated numerically.

For any given spacing v, the most severe test of the solution method is for small ε. Illustrative comparisons between the present results and those from the numerical solutions of [2] are shown in Table 1. Inspection of the table shows that with only a moderate number of terms in the functional relationship (7), the present method of solution can reproduce the results of the numerical solution to high accuracy. Furthermore, for values of M at which the results are insensitive to further increases in M, the results were also insensitive to the number of points P (provided, of course, that $P \geqslant M$). This information can be employed to reduce the time required to obtain a solution.

Two-dimensional systems. Next, consider a pair of abutting square plates as illustrated at the upper right of Fig. 1. The general case where the plates have different temperatures T_1 and T_2 and the environment contains blackbody radiation at T_e can be synthesized from solutions of the fundamental case in which $T_1 = 1$, $T_2 = T_e = 0$. The plate surfaces are gray diffuse emitters and reflectors with emittance ε. The governing integral equations for the radiosity distributions $B_1/\varepsilon\sigma = \beta_1$ and $B_2/\varepsilon\sigma = \beta_2$ are

$$\beta_1 = 1 + (1 - \varepsilon) \int_0^1 \int_{-\frac{1}{2}}^{\frac{1}{2}} \beta_2 \, K \, dy \, dx_2,$$

$$\beta_2 = (1 - \varepsilon) \int_0^1 \int_{-\frac{1}{2}}^{\frac{1}{2}} \beta_1 \, K \, dz \, dx_1 \qquad (8)$$

where $\beta_1 = \beta_1(x_1, z)$, $\beta_2 = \beta_2(x_2, y)$, and $K(x, y)$ is given by equation (4–28) of [1]. In accordance with equation (2), and accounting for symmetry, one proposes

$$\beta_1 = C_{11} + z(C_{12} + C_{13} x_1^2 + C_{14} x_1^4) + z^2(C_{15} + C_{16} x_1^2 + C_{17} x_1^4) + \ldots \qquad (9)$$

and analogously for β_2. Also, by taking limits as y and z approach zero, it can be shown that $C_{11} = [1 - (\frac{1}{4})(1 - \varepsilon)^2]^{-1}$ and $C_{21} = (\frac{1}{2})(1 - \varepsilon)C_{11}$.

In applying the solution method, all of the participating integrals were evaluated numerically. Computations were performed for various numbers of terms M_1 and M_2 in the functional forms for β_1 and β_2; in addition, the number of linear algebraic equations P was also varied. It was found that the results were relatively insensitive to $P (\geqslant M_1 + M_2)$. For purposes of comparison, a finite-difference solution was

Table 1. Radiosity distributions $\beta(x)$ for $\varepsilon = 0{\cdot}1$, first computational experiment

v	M	x					
		0	0·1	0·2	0·3	0·4	0·5
1·0	2	1·642	1·637	1·620	1·592	1·554	1·504
	3	1·644	1·638	1·620	1·591	1·553	1·508
	Ref. [2]	1·644	1·638	1·620	1·591	1·553	1·508
0·05	2	9·694	9·444	8·695	7·447	5·699	3·452
	3	8·958	8·929	8·739	8·088	6·473	3·191
	4	9·092	8·984	8·651	7·986	6·541	3·126
	5	9·082	8·984	8·661	7·984	6·536	3·120
	Ref. [2]	9·08	8·98	8·66	7·98	6·54	3·13

performed using the linear equation subroutine of the Control Data 6600.

Representative comparisons between the β distributions from the two solution methods are presented in Figs. 1 and 2, respectively for $\varepsilon = 0{\cdot}9$ and $\varepsilon = 0{\cdot}5$. Distribution curves are shown for $x = 0{\cdot}05$ and $x = 0{\cdot}35$ for both β_1 and β_2. (For $\varepsilon = 0{\cdot}9$, β_1 is essentially unity and is not plotted.) The results from the orthonormalization least squares solution are for $M_1 = M_2 = 13$ and $P = 90$, while those for the finite-difference solution are for a total of 200 nodal points, 100 on each surface. Generally good agreement prevails, except at small values of y and z, where the finite-difference solution is in error. Additional nodal points would have to be added to the finite-difference grid to insure accurate results in the neighborhood of the interface between the plates. The distribution curves for the least squares solution are slightly wavy, probably due to the high-degree polynomials employed.

Local and overall heat transfer results were also computed. The local heat fluxes q_1 and q_2 are determined from the local radiosity by employing equation (5). The overall heat transfer rates Q_1 and Q_2 are given by $Q = q\,dA$, the inte-

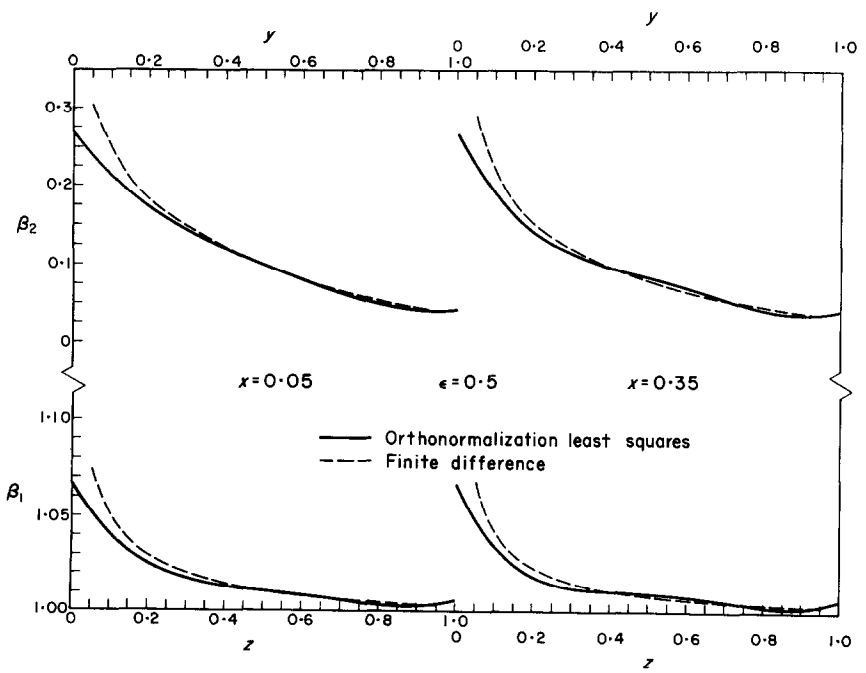

FIG. 2. Radiosity distributions, second computational experiment, $\varepsilon = 0{\cdot}5$.

grations being performed analytically in the case of the least squares solution and numerically in the case of the finite-difference solution.

Results for Q_1 and Q_2 are listed in Table 2. In the (a) and (b) parts of the table, it is seen that the overall heat transfer is little influenced by the number of terms $\tilde{M} = M_1 + M_2$ of the functional representation and by the number of points P used to generate the linear algebraic equations. The results of the finite-difference solution, part (c), are in good agreement with those of parts (a) and (b). Part (d) of the table gives the Q_1 and Q_2 values for the gross model in which B_1 = constant and B_2 = constant.

For the conditions of Figs. 1 and 2, the computation times of the least squares and finite-difference methods are essentially the same, about 20 s per case on the CDC 6600. However, it should be mentioned that the computation time for the least squares method can be substantially diminished, for instance, by reducing P or by analytical integration of some of the participating integrals.

Table 2. Overall heat transfer results, second computational experiment

(a) $P = 90$

	$\varepsilon = 0{\cdot}9$		$\varepsilon = 0{\cdot}5$	
$\tilde{M}$	Q_1/σ	Q_2/σ	Q_1/σ	Q_2/σ
14	0·8948	0·1660	0·4916	0·05294
20	0·8953	0·1632	0·4926	0·05165
26	0·8955	0·1627	0·4928	0·05136

(b) $\tilde{M} = 26$*

	$\varepsilon = 0{\cdot}9$		$\varepsilon = 0{\cdot}5$	
P	Q_1/σ	Q_2/σ	Q_1/σ	Q_2/σ
24*	0·8953	0·1633	0·4925	0·05172
90	0·8955	0·1627	0·4928	0·05136
132	0·8955	0·1627	0·4928	0·05133

(c) Finite-difference solution

	$\varepsilon = 0{\cdot}9$		$\varepsilon = 0{\cdot}5$	
Nodes	Q_1/σ	Q_2/σ	Q_1/σ	Q_2/σ
50	0·8939	0·1837	0·4903	0·05850
98	0·8943	0·1777	0·4909	0·05650
162	0·8946	0·1743	0·4913	0·05535
200	0·8947	0·1731	0·4914	0·05495

(d) Gross calculation, B_1 = constant, B_2 = constant

$\varepsilon = 0{\cdot}9$		$\varepsilon = 0{\cdot}5$	
Q_1/σ	Q_2/σ	Q_1/σ	Q_2/σ
0·8968	0·1621	0·4949	0·05052

* Note that C_{11} and C_{21} are fixed in advance.

REFERENCES

1. E. M. SPARROW and R. D. CESS, *Radiation Heat Transfer*. Brooks/Cole, Belmont, California (1966).
2. E. M. SPARROW, J. L. GREGG, J. V. SZEL and P. MANOS, *J. Heat Transfer* **83**, 207–214 (1961).